Cellulose (2012) 19:1945–1956
DOI 10.1007/s10570-012-9761-x

ORIGINAL PAPER

A fundamental investigation of the microarchitecture and mechanical properties of tempo-oxidized nanofibrillated cellulose (NFC)-based aerogels

Teresa Cristina Fonseca Silva · Youssef Habibi · Jorge Luiz Colodette · Thomas Elder · Lucian A. Lucia

Received: 30 March 2012 / Accepted: 4 August 2012 / Published online: 15 August 2012

Abstract Freeze-dried nanofibrillated cellulose based-aerogels were produced from cellulosic pulps extracted from *Eucalyptus urograndis*. Nanofibers were isolated under high pressure and modified with TEMPO-mediated oxidation and/or hydroxyapatite (HAp) to observe potential changes in mechanical properties. Two degrees of oxidation (DO), 0.1 and 0.2, were achieved as measured by conductimetric titration. Oxidized and non-oxidized samples were modified with HAp at a ratio of HAp:cellulose of 0.2:1. Morphology (FE-SEM), pore size, surface area, and mechanical properties were obtained to characterize the produced aerogels. The results clearly demonstrate a homogeneous morphology for aerogels fabricated with oxidized cellulose nanofibers. The nature of water present in the material was measured using time domain-nuclear magnetic resonance spectroscopy (TD-NMR) and demonstrated that it played a key role in the development of the porous and uniform microarchitecture. TEMPO-mediated oxidation and the addition of HAp resulted in aerogels with high mechanical strength as demonstrated from an increase from approximately 75–200 kPa in compressive strength when reduced to 50 % of their original height. However, the contribution of oxidation to the mechanical properties was more pronounced than the addition of HAp. In general, the density of the aerogels varied from 0.008 to 0.011 g/cm^3 in which slightly lightweight aerogels were produced by increasing the degree of oxidation, whereas the incorporation of HAp as a modifying agent for potential bio-based tissue scaffolding matrices did not significantly contribute to higher densities.

Keywords NFC · Aerogels · TEMPO · Hydroxyapatite

T. C. F. Silva · J. L. Colodette
Departamento de Quimica, Universidade Federal de Viçosa, Viçosa, MG 36570-000, Brazil

T. C. F. Silva · Y. Habibi · L. A. Lucia (✉)
Laboratory of Soft Materials & Green Chemistry, Department of Forest Biomaterials, North Carolina State University, Raleigh, NC 27695-8005, USA
e-mail: lalucia@ncsu.edu

Present Address:
Y. Habibi
Laboratory of Polymeric and Composite Materials, Center of Innovation and Research in Materials and Polymers (CIRMAP), University of Mons, Place du Parc 23, 7000 Mons, Belgium

T. Elder
Southern Research Station, Utilization of Southern Forest Resources, USDA Forest Service, 2500 Shreveport Highway, Pineville, LA 71360-2009, USA

Introduction

Aerogels are highly porous materials characterized by an extremely low solids content and considerably

lightweight nature giving rise to a highly open microstructure with lots of connected pores, hence ultralow density, high strength, and have very good dimensional stability. More specifically from a nanoscopic perspective, the extensive interconnectivity provides a stable three-dimensional network with pore diameters typically being on the order of 10–100 nm (Liebner et al. 2008). These extremely open materials ($\sim 97 + \%$ air) have led to the development of wide range of materials that are used in a variety of applications such as storage media for gases, filter materials, carriers for catalysts, scavengers for dust particles, shock absorbers, and heat and sound insulators (Burchell et al. 2001).

Although aerogels can be prepared from an extensive array of materials, new precursors that are considered more ecofriendly are nowadays emerging. A particular promising candidate addressing the aforementioned trend is cellulose. This material is considered to comprise the newest and most renewable generation of aerogels. What is remarkable about cellulose aerogels is that the solution structure of the cellulose is largely retained while it is then transferred to the solid state, resulting in a material having densities down to 0.05 g cm^{-3} and surface areas of up to 280 m^2 g^{-1} (Liebner et al. 2008).

Cellulose is a natural polysaccharide that is the most abundant, sustainable material in the biosphere, but it has not received the commensurate attention for novel material applications as its availability would suggest; however, with pressing economic and environmental concerns based on dwindling petroleum supplies, it has been nevertheless slowly gaining ascendancy as a raw material for a number of market applications that have already been listed (vide supra). The excellent mechanical properties of cellulose have led to the use of cellulose nanofibers as reinforcing materials, a concept that is currently garnering a tremendous level of attention in the materials community (Dufresne et al. 2000). Cellulose nanofibers or nanofibrillated cellulose (NFC), obtained by mechanical disintegration of cellulose fiber along their principal axis, are high aspect ratio fibers with diameters ranging from 3 to 100 nm depending on their origin. NFCs possess very high mechanical properties in addition to the conventional advantages of natural fibers, such as low cost, renewability, low density and biodegradability. Hence, NFCs are widely used as a reinforcing medium in polymeric composites to improve the bulk mechanical properties. Furthermore, the foam-forming capability of NFC is a very interesting trait that makes it highly suitable as a precursor for aerogel preparation. Indeed, gel-like water suspensions of NCF can be easily converted to ultra-lightweight porous materials after controlled water removal. NCF-based aerogels are therefore gaining increased attention because they can be tuned to have physical properties comparable to those produced from inorganic counterparts such silica, alumina, or carbon (Innerlohinger et al. 2006).

One way of obtaining NFC-based aerogels is by carefully drying the wet gel state of the NFC using either freeze drying or supercritical drying to maintain the integrity of the micro-porous structure and limit "capillary effect" shrinkage of the aerogel (Paakko et al. 2008). Similarly, Heath and Thielemans have also reported the production of aerogels based on cellulose nanowhiskers which are a class of nanomaterials that may properly be described as highly crystalline rod-like cellulosic particles (Heath and Thielemans 2010). These cellulose nanowhiskers were blended with clay and processed to produce a hybrid aerogel (Gawryla et al. 2009). There have been several reports recently that have highlighted new synthetic procedures and the novel properties of cellulose-based aerogels (Sehaqui et al. 2011a, b). These latter methods have shown the incredible delivery of high surface area, porosity, and ultra-light weight density. In addition, these methods have pointed to the preservation of intramolecular hydrogen bonding. Hydrogen bonding has been recognized to be an important component in the development of many higher organized structures (Archer et al. 2001). In fact, it is one of the most important parameters controlling cellulosic crystallinity. Thus, the location and state of water within the cellulosic nanofibers may play an important role on the drying process consequently impacting the final morphology of the aerogel. Entrapped water within the nanofibers is subject to a variety of interactions and understanding these interactions may be necessary to controlling the properties of the final material (Felby et al. 2008) and therefore targeted as one of the objectives of this study.

Tuning the properties of any chemical assembly to obtain specific applications may require chemical tweaking of the existing structure(s) (Aulin et al. 2010). Thus, introducing modifications within cellulose is an interesting approach for higher value-added

products. One common modification is the catalytic oxidation of cellulose using 2,2,6,6-tetramethylpiperidine-1-oxy (TEMPO) to introduce functionalities such as aldehyde and carboxyl groups and thus derive new industrial uses (Bragd et al. 2004). Oxidation in cellulose induced by the application of TEMPO selectively converts the hydroxymethyl groups (C_6 groups) to carboxylic groups, thus imparting a net negative surface charge to the nanofibers. The use of this green chemical route has been attracting a number of investigations since the first reports of de Nooy et al. (de Nooy et al. 1995) which showed that only the hydroxymethyl groups of polysaccharides were oxidized, whereas the secondary hydroxyls remained unaffected. In the case of cellulose nanofibers, several reports have also demonstrated that the oxidation occurs only at their surface without any effect on their morphology (Habibi et al. 2006; Isogai et al. 2011). For instance, improvements in the physical properties of pulp-based handsheets have been observed when TEMPO-oxidized pulps were used because inter-fiber bond is enhanced via the availability of additional hydrogen bonding pathways.(Saito and Isogai 2006) Also, when dispersed in water, oxidized NFC does not flocculate, but instead becomes a homogeneous mixture that may serve as a platform for the formation of highly viscous hydrogels that can be further converted into resistant aerogels.

The attractiveness of the current approach lies in the use of TEMPO as an oxidizing agent for the NFC post-homogenization. Typically, the use of TEMPO before cellulose homogenization will not lead to a homogeneous distribution of carboxylic acid functionalities within the cellulose matrix, although it significantly improves the mechanical processability of the cellulose (Besbes et al. 2011). The current approach of applying TEMPO to NFC post-homogenization is able to provide an oxidized NFC that is extremely amenable to a very efficient subsequent aerogelation stage that as will be shown controllably delivers high porosity and mechanically-tunable aerogels.

Another alternative approach for cellulose modification for enhanced mechanical and/or chemical properties that has been unexplored until the present, is the use of hydroxyapatite (HAp), ($Ca_{10}(PO_4)_6(OH)_2$). HAp is a mineral-based compound that constitutes a large fraction of dental tissue and therefore has mechanical and biochemical properties that make it attractive for applications such as artificial bones and scaffolds for tissue engineering (Hong et al. 2006). A range of features has been obtained after HAp introduction to cellulose such as high mechanical properties, good porosity, high water holding capability, excellent biocompatibility, and bone-bonding ability (Wan et al. 2006). Phosphorylated bacterial cellulose nanofibers have been shown to be an efficient template for the nucleation and growth of HAp (Wan et al. 2009). Furthermore, a biomimetic approach was used to design and synthesize bacterial cellulose/HAp nanocomposites by in vitro cultivation of calcium-deficient HAp via dynamic simulated body fluid treatments. The presence of calcium-deficient HAp crystals on bacterial cellulose surfaces resulted in increased cell attachment. Thus, the resulting nanocomposites showed a great potential for bone healing applications (Zimmermann et al. 2011). Cellulose composites can be formed in a variety of shapes to provide biocompatible products. However, many studies have been carried out to address the limitation of using cellulose as an artificial bone scaffold or substitute because it does not directly bond to it (Kwak et al. 2010).

The overall aim of this work was to produce, adequately characterize, and begin to explore the mechanical properties of aerogels that were generated as post-homogenized TEMPO-oxidized NFC aerogels and/or with HAp incorporation, and a combination of both. The produced aerogels were characterized according to their morphology (FE-SEM) and bound water followed by subsequently reporting their unique mechanical properties.

Materials and methods

Materials

Potassium hydroxide (99 %), hydrogen peroxide (30 %), acetic acid (99.5 %), hydroxyapatite, sodium hydroxide (0.01 N), and hydrochloric acid (0.01 N), TEMPO, sodium bromide, sodium hypochlorite solution were purchased from Sigma-Aldrich and used without further purification unless otherwise noted.

Isolation of nanofibrillated cellulose (NFC)

The starting cellulosic material was a hardwood (*Eucalyptus urograndis*). Extractives-free sawdust of

the hardwood samples was subjected to delignification with peracetic acid (15 % concentration) to yield holocellulose. Subsequently, hemicelluloses were removed by using KOH (24 %) at room temperature. Cellulose fibers left were washed several times and allowed to swell for 1 day in deionized water until a w/v ratio of 2.0 % was achieved. Next, the sample was dispersed in a Waring blender for 5 min to obtain a uniform fiber suspension. A NFC aqueous gel was obtained by passing the fiber suspension through a high pressure homogenizer (15MR two-stage Manton-Gaulin homogenizer—APV, Delavan, WI, USA) at approximately 1 % solids content. The operating pressure was maintained at 55 MPa and the suspension was collected after 20 passes through the homogenizer and stored at 4 °C until needed.

NFCs modifications

TEMPO-mediated oxidation of NFCs

A sample of nanofibrillated cellulose (2 g) was suspended into 250 mL of deionized water followed by addition of TEMPO (0.058 g, 0.095 mmol) and sodium bromide (0.635 g, 1.57 mmol). The TEMPO-mediated oxidation was started by adding the desired amount of the 1.24 M NaClO solution (1.6—5.0 mmol NaClO per gram of cellulose). The pH of the mixture was maintained at 10 at room temperature by adding 0.5 M NaOH while stirring. After 45 min, the oxidation was terminated by adding several drops of methanol and the pH was adjusted to 7 with 0.5 M HCl. The oxidized samples were recovered by centrifugation and then dialyzed against deionized water.

NFCs modification by the incorporation of hydroxyapatite (HAp)

HAp aqueous solutions (pH $\sim$4) were prepared at a concentration of 0.5 mol L^{-1} and a volume of 1.0 mL of each solution was added to oxidized and non-oxidized NFCs after centrifugation to reach a mass ratio for HAp:cellulose equal to 0.2:1.

Preparation of NFC-based aerogels

After removing the excess of water by centrifuging the NFC suspension, the aqueous gels, with the same water to NFC weight ratio, were placed on cylindrical molds and quickly plunged in liquid nitrogen at a temperature of ca. 83 K. The frozen samples in the mold were transferred to a pre-cooled glass bottle and subjected to freeze drying under vacuum for 30 h.

Conductimetry

Conductimetric titration was used to determine the carboxyl content of oxidized NFC. The samples (30, 50 and 100 mg) were suspended into 15 mL of 0.01 M hydrochloric acid solutions and stirred for 10 min. Afterwards, the suspensions were titrated with 0.01 M NaOH and titration curves were generated (Fig. 2). From the curves, it was possible to calculate the amount of carboxyl groups and therefore the degree of oxidation (DO) according to accepted procedures for these biomacromolecules (da Silva Perez et al. 2003)

$$DO = \frac{162C(V_2 - V_1)}{w - 36C(V_2 - V_1)}$$

where C is the NaOH concentration (mol L^{-1}), V_1 and V_2 are the initial and final amount of NaOH (L), respectively, based on the plateau of the curve, and w (g) is the mass of the oven-dried sample.

Infrared spectroscopy

FT-IR spectroscopy was performed on a Thermo Nicolet NEXUS 670 FT-IR spectrophotometer. Spectra were obtained after the accumulation of 128 scans which had a resolution of 4 cm^{-1} over the range of 4,000–650 cm^{-1}. Oxidized NFCs were converted to their acid forms by ion exchange to displace the carboxyl absorption band toward higher energy wavelengths and thus eliminate any interference with the band of absorbed residual water (1,640 cm^{-1}).

Scanning electron microscopy (SEM)

The morphology of the hydrogels was monitored by field emission scanning electron microscopy (FE-SEM) using a JEOL 6400F microscope operated at an accelerating voltage of 5 kV, a working distance of 15 mm, and a 30 μm objective aperture. A small hydrogel-sized sample was affixed onto a small piece of conductive carbon tape, mounted on the support, and then sputtered over with an approximately 25 nm-thick layer of gold/palladium (60/40).

BET measurements

Specific surface area and pore volume of the cellulose aerogels analysis were carried out using the Brunauer–Emmett–Teller (BET) nitrogen adsorption/desorption method on a HORIBA SA-9601-MP. The samples were degassed under flowing UHP-grade nitrogen for 2 h at a temperature of 100 °C before testing. The experiment was done in triplicate.

Physical properties—rheology, pore size, and density

Load and strain (deformability) of the aerogels were determined by compression testing. Gels were cut into cylinders (~23.5 mm in height) and compressed to 50 % of their original height between plates using a universal testing machine (Model 5565, Instron Engr. Corp., Canton, Mass., U.S.A.) operated using Bluehill® software version 2.0 (Instron Engr. Corp.). A 5 kN load cell was used for all samples. Rheological measurements were done in duplicate. Pore size distribution of the cellulose aerogels was determined in triplicate by differential scanning calorimetry (DSC) using previously established methods (Park et al. 2006). Apparent density of the aerogels was evaluated from mass (±0.1 mg) and geometric dimensions while making sure to avoid deformation of the soft specimens. Measurements were done in triplicate.

NMR acquisitions

A Bruker mq20-Minispec (20 MHz proton resonance frequency) operating at 40 °C was used for the NMR analyses of the aerogels modified with TEMPO and the control. Additionally, filter paper was used for the assignment of water pools (Felby et al. 2008). A Carr-Purcell-Meiboom-Gill (CPMG) pulse sequence was used to determine the transverse (T_2) relaxation times through the transformation method CONTIN, which consisted of 500 echoes, a 5 s recycle delay, and a pulse separation of 0.05 ms.

Results and discussion

Suspensions of nanofibrillated cellulose (NFC) were generated from non-oxidized (DO = 0) and TEMPO-oxidized (DO = 0.1 and 0.2) samples with or without the addition of HAp. In sum, six NFC-based aerogel samples were produced that were further characterized according to their density, surface area (BET), morphology (FE-SEM), and their rheological properties.

NFC modification and drying

The TEMPO-mediated oxidation of NFC resulted in two distinct DOs as measured by conductimetric titrations (Fig. 1) and confirmed by FTIR (they are shown to demonstrate the sensitivity in the variation of the measurements of the DOs). By varying the amount of the primary oxidizing agent, c.a. sodium hypochlorite NaOCl, two (2) DOs of 0.1 and 0.2 were achieved. The maximum DO of 0.2 achieved could not be superseded by any additional amounts of NaOCl indicating a threshold in the overall concentration of carboxylic acid groups on the NFC. It is worth noting that the non-oxidized sample had a miniscule DO of 0.03 (again measured by conductimetry, showing the sensitivity of this measurement), a residual content that likely arose from adventitious oxidation during the delignification of wood through the use of peracetic acid.

Resulting NFCs were then analyzed by FTIR (as alluded to above, vide supra) and the spectra of the oxidized and non-oxidized samples are shown in Fig. 2. It is possible to notice the changes in bands due to the selective TEMPO oxidation of the hydroxyl group at C-6 position in the glucose ring. The band at 1,720–1,740 cm^{-1} on the FT-IR spectra confirms the presence of carboxylic acid groups, and its intensity can be correlated to the level of DO achieved to confirm the conductimetric titrations shown in Fig. 1. For non-oxidized NFC (DO ~0.03), it was confirmed that the raw samples have much lower acid contents from observing the intensity of the acid band in relation to the characteristic cellulose band near 1,420 cm^{-1} (C–O stretching).

Once TEMPO-oxidation of NFC suspensions was successfully accomplished, HAp was added as a physical modification agent at a weight ratio of HAp:cellulose of 0.2:1. Finally, the resulting aqueous suspensions of NFC were dipped in liquid nitrogen and directly freeze-dried to remove the water content.

Homogeneously oxidized cellulose nanofibers in water were obtained after the TEMPO-mediated oxidation. The TEMPO-mediated oxidation done after the homogenization of the fibers allowed the carboxyl

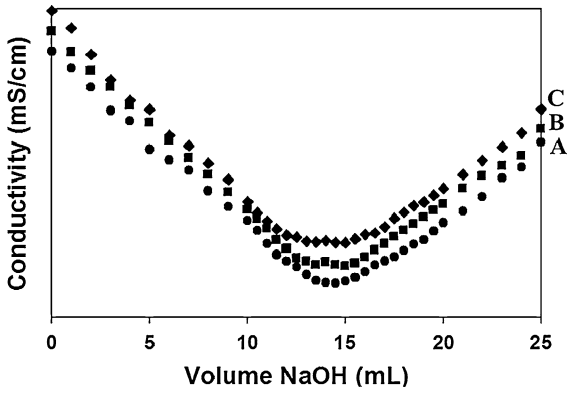

Fig. 1 Conductimetric titration curves of TEMPO-mediated oxidized NFC with different DOs: non-oxidized (*Circle*), *A*, oxidized with DO = 0.1 (*Square*), *B*, oxidized with DO = 0.2 (*Diamond*), *C*

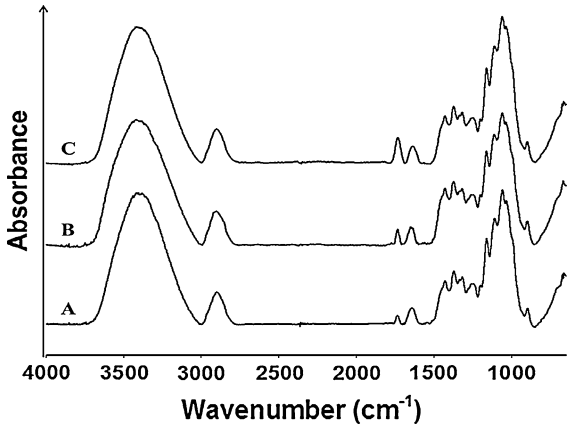

Fig. 2 FTIR spectra of the NFC generated in this study: non-oxidized, *A*, TEMPO-mediated oxidation to DO = 0.1, *B*, and to DO = 0.2, *C*

groups to be homogenously distributed along the fibers resulting in the observed homogenous dispersion, in contrast to what has been observed previously where the oxidation was carried out before the disintegration (Hoepfner et al. 2008; Saito et al. 2007). Although previous fibers were individualized, the oxidation before homogenization occurred only at accessible surfaces; thus, part of the nanofibrillar surfaces were not oxidized thus presenting a more heterogeneous distribution on the fibers and uneven dispersion as witnessed in past systems (vide supra).

One of the most common challenges in aerogel preparation is the drying process because direct drying of hydrogels typically induces total collapse of the porous network structure because of the capillary forces resulting from the strong surface tension of leaving water. As a result, severe shrinkage of the aerogels occurs, which lowers the porosity and increases the density. It was found in the present study that light-weight sponge-like aerogels were produced with no significant collapse or shrinkage and the porosity of the aerogels was virtually maintained. In comparison to past accounts, these specific aerogels possess equivalent if not superior physical properties to those of their predecessors. Figure 3 illustrates the photographs of the cylindrical-shaped aerogels produced from freeze-drying. As can be observed, the integrity of the aerogel has not been compromised upon drying. Non-oxidized NFC-based aerogel itself was slightly brittle in comparison to the oxidized samples.

Pore size, surface area, pore volume, and density of the aerogels

Recently, many studies have analyzed the influence of freeze-drying conditions as well as NFC concentration on cellulose-based aerogel fabrication (Aulin et al. 2010; Hoepfner et al. 2008; Suh and Park 1996). In the present work, the same NFC suspension concentration (0.8 wt%) and the same drying conditions were applied throughout and consequently any changes on surface area, pore volume, pore size, and density can be uniquely attributed to the chemical/physical modifications of the aerogels.

Table 1 gathers the collected results for the aerogels obtained from different conditions previously described.

Density determination was carefully carried out by weighing the same amounts of NFC suspensions before placing them in vials for further freeze-drying. Thus, it was possible to note a variation in the volume of the aerogels after drying. Aerogels presented quite low densities varying from 0.008 to 0.0108 g cm^{-3} which compare extremely well with previous results (Felby et al. 2008).

It can be observed that a higher degree of oxidation provided aerogels with lower densities and more open structure as the pore size increased from 29.1 up to 47.4 nm, which can be related to the enhanced electrostatic repulsion between the nanofibers in the suspension because of the presence of negatively charged carboxylic groups at their interfaces.

After the addition of HAp, the densities slightly increased as expected, but the aerogels maintained the

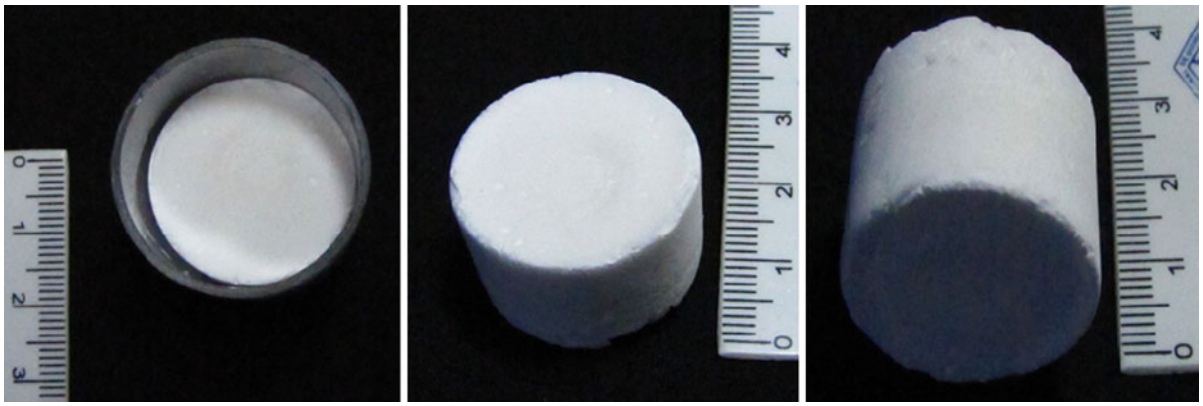

Fig. 3 Macro structures of cellulose aerogels obtained after the freeze-drying (*Left*: the cylindrical mold used during freeze-drying)

Table 1 Surface area, pore volume, and density of the NFC aerogels (AGs)

Sample	Surface area (m^2/g)	Pore volume (cm^3/g)	Pore size average (nm)	Density (g/cm^3)
AG DO = 0	18.4	0.014	29.1	0.0098
AG DO = 0.1	14.6	0.008	35.8	0.0085
AG DO = 0.2	13.8	0.007	47.4	0.0080
AG DO = 0 + HAp	19.8	0.016	28.5	0.0108
AG DO = 0.1 + HAp	16.5	0.010	33.4	0.0103
AG DO = 0.2 + HAp	16.9	0.010	39.1	0.0105
Coefficient of variation[a]	±2.5 %	±12.5 %	±9.0 %	±4.6 %

[a] Higher value of coefficient interval for each parameter

same trend in regard to the pore volume showing that HAp did not screen out the interactions between the fibers.

Because of the narrow range of density values for all samples, the porosity was very high (from 99.3 to 99.5 %), where porosity, ϕ, defined as $\phi = 1 - (\rho/\rho_s)$ and ρ and ρ_s are the densities of the aerogel and the cellulose fibers, respectively.

The specific surface areas of the resulting aerogels are in agreement with those reported for freeze-dried NFC aerogels using liquid nitrogen for cooling (Aulin et al. 2010; Paakko et al. 2008). Higher surface areas have earlier been found for cellulose aerogels that were rapidly cooled with propane before freeze-drying (Gavillon and Budtova 2007; Paakko et al. 2008). Differences in the surface area of the aerogels can be noticed between oxidized and non-oxidized aerogels with or without HAp. As expected, the average pore size of the aerogels has an inverse response compared to surface area. It is likely that the oxidized aerogels have a slightly higher pore size by virtue of the "templating" effect of the acid functionalities. In general, acid hydrogen bonding can organize water molecules to organize a higher order crystalline pattern and provide a more ordered environment. It has been already observed that acid conditions can tailor the mesoporous cavities within inorganic aerogels by controlling the degree of metal oxide particle crosslinking (Suh and Park 1996). In the organic aerogels, we conjecture a general acid effect that is modulated by the carboxylic acid groups in which by virtue of an extensive hydrogen-bonding network the cavities formed are much larger because the overall physical stresses can be more evenly distributed. In the non-oxidized samples, the cavities that are formed are smaller because the strain cannot be as easily distributed because of the lack of a templating effect offered by the general acid effect of the C_6 acid groups. This hypothesis was supported by the results obtained from time-domain low field NMR studies of both the oxidized and non-oxidized NFC samples (vide infra). The pore size average revealed differences between samples, although all of them were classified as mesoporous according to IUPAC (2–50 nm).

Morphology, water nature, and rheological properties

It is worth mentioning that the use of the NFC suspension does form a hydrogel-like network. However, the oxidized samples provide more homogeneous and more viscous hydrogels, thus providing empirical evidence to the formation of a homogeneous aerogel network having a well aggregated-like structure.

Previous work has revealed that the homogenization of pre-TEMPO-mediated oxidized fibers can more easily disintegrate cellulose fibers into a microfibrillated suspension than using mechanical treatment alone (Saito et al. 2006). However it is commonly believed that the carboxyl groups cannot be homogenously distributed in these fibers compared (Okita et al. 2010) to the post-oxidized nanofibers shown here.

The aerogels presented diverse macroscopic morphologies, especially when contrasting samples with different DOs. It became clear that the samples with higher DOs displayed a more organized structure with homogenous distribution of the pores, revealing a more hierarchical order in the open-porous cellulose network (Fig. 4).

The higher the degree of oxidation (DO = 0.2) of the aerogels, the more homogeneous the morphology. Obviously, the generation of a homogenous, isochoric microporous architecture depended heavily on avoidance of the capillary effect induced by water surface tension. Thus, to better understand the cause for the homogeneous morphology of the oxidized samples, the nature of water present in the cellulose aerogels was studied by the use of time domain low field NMR. This technique has been used for examination of wood, paper, and cellulose and consists of the application of a radio-frequency pulse that perturbs the nuclei from their resting state, inducing a magnetic field. The time required for the decay of this magnetic field can be measured, being described by the spin–lattice relaxation time (T1) and the spin–spin relaxation time (T2) (Elder et al. 2006). The water contained within cellulose can be subdivided into categories and the effects of the interaction of a specific type of water with cellulose will lead to changes in the physical properties of cellulose, including mechanical properties. Relaxation times are affected by surface areas and there might exist strongly hydrogen bonded water at hydrophilic interfaces.

Relaxation time distributions for the aerogels samples are shown in Fig. 5. The moisture level was right below the fiber saturation point. Moisture contents were obtained for the samples after conditioning in a dessicator over deionized water. Assignments were done for peaks based on previous work (Felby et al. 2008).

Aerogels based on oxidized samples (DO = 0.1 and AG DO = 0.2) exhibited two similar peaks. The first peak at times of 0.78 and 0.67 ms and a second one at 13 and 14 ms for lower and higher degrees of oxidation, respectively. The non-oxidized sample showed a major peak at 1.13 ms similar to the filter paper (1.32 ms). The signal strength is proportional to the water content and, in this case, the highest peak was attributed in all cases to the less tightly associated secondary bound water localized in the surface of nanofibers, even though extended times can be found for non-oxidized samples.

The rationale for the time shifting observed between oxidized and non-oxidized sample/paper filter samples may be attributed to the pore size of the cellulose matrix and the water-cellulose interactions. Extended relaxation times as found for non-oxidized samples were attributable to higher moisture contents. The presence of the carboxylic acid functionalities in the oxidized samples contributed to a higher interaction between the cellulose chains and water, thus reducing the moisture content. Therefore, it is reasonable to postulate based on earlier arguments (vide supra) that such an interaction would be able to provide a well-organized, more homogeneous, and hence uniformly porous morphology as already indicated because nearly all water content in such aerogels is weakly associated with the nanofiber structure.

A review of the SEM images demonstrates the aggregation of HAp in the cellulose fibers of the aerogels as observed in Fig. 6. Overall, HAp influences the localized aerogel micro-architecture as observed in Fig. 4. The morphology of the non-oxidized NFC-based aerogel without HAp was more or less intact even after the addition of HAp. However, for both DO levels of TEMPO-oxidation, HAp affects the morphology creating a closer network structure which may have been facilitated by the presence of negatively charged acidic groups available on the cellulose structure. This observation is corroborated by the previous results obtained by Zimmermann et al. (2011) who showed that the presence of negative

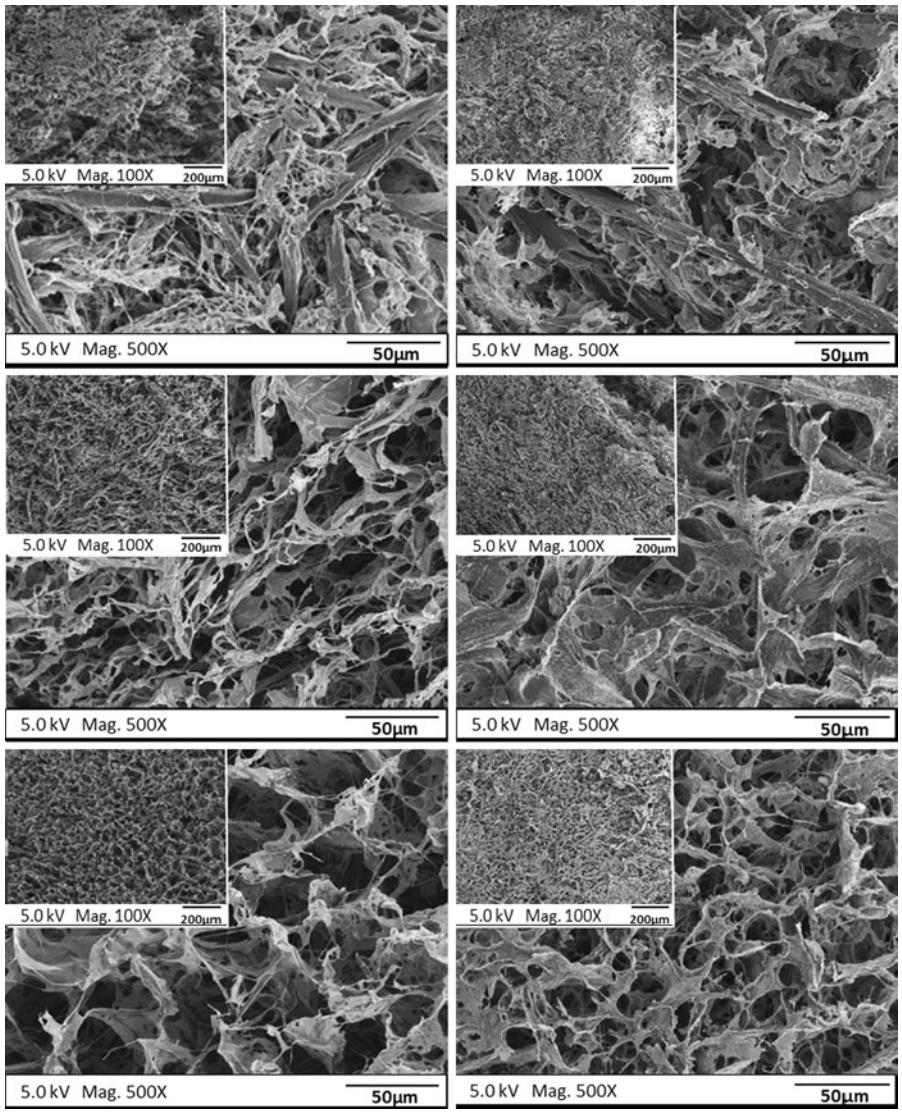

Fig. 4 SEM of the aerogels based on NFC having different degree of oxidation without the addition of HAp (*Left*) and with the addition of HAp (*Right*). From the top to the bottom: DO = 0, 0.1, and 0.2

charges provided by carboxymethly cellulose used in their work in combination with bacterial cellulose nanofibers were necessary for efficient HAp growth and attachment. Thus, the benefit of using TEMPO-mediated oxidation to introduce negative charges is therefore clearly supported.

The resulting aerogels were then analyzed for changes in their mechanical properties by measuring the force applied to compress the samples to 50 % of their original length (Fig. 7). After compression, the oxidized aerogels (without HAp) were able to slightly recover approximately 65 % of the original length, whereas the non-oxidized ones were able to attain only 55 % of the original length. The addition of HAp to the aerogels did not contribute as much as its absence on the recovery of the aerogels. Oxidized aerogels were able to achieve 55 % of their original length, but no significant height recovery was noticed for the non-oxidized aerogels.

Figure 7 shows the effect of the TEMPO-oxidation: it leads to a more highly compression-resistant sample. Ostensibly, the addition of HAp to all three oxidized

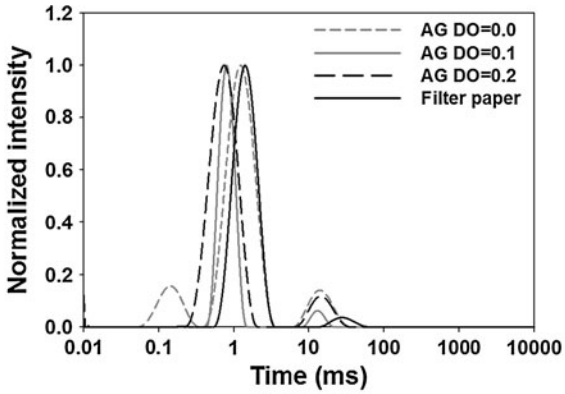

Fig. 5 Relaxation time distributions for saturated non-oxidized and oxidized cellulose aerogels and filter paper

samples increased the resistance of the NFC aerogels as well. The synergistic effect of oxidation and HAp on the resulting aerogels were able to increase their resistance by up to three fold. Although the oxidation effect was more pronounced, the HAp addition played a crucial role to enhance the resistance of these materials.

A combination of HAp and TEMPO-mediated oxidized cellulose nanofibers would therefore be expected to offer striking features such as high mechanical properties, excellent biocompatibility, and bone-integrating ability. The current work is the first of its kind to present data on HAp-NFC composites to form aerogels that provide high mechanical performance as an alternative for bone tissue engineering fields.

According to the obtained results, the addition of HAp in all oxidized and non-oxidized samples provide significant strength to the NFC-based aerogels. This fact supports the supposition that NFC that is a priori modified by TEMPO, possesses viscoelastic properties that are significantly improved by addition of HAp. Even though TEMPO-oxidized aerogels have demonstrated significant advantages for strength improvement, the incorporation of HAp to modify the aerogels is an alternative to additionally improve mechanical properties of the aerogels.

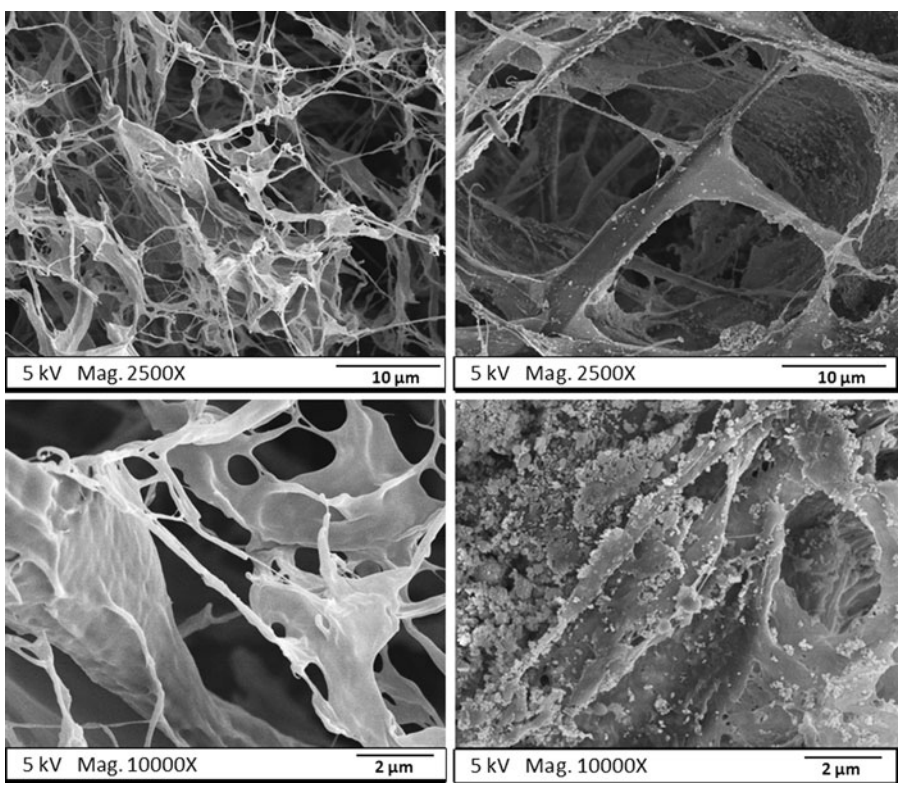

Fig. 6 SEM images of the aerogels based on NFC with DO = 0.2 without the addition of HAp (*Left*) with the addition of HAp (*Right*)

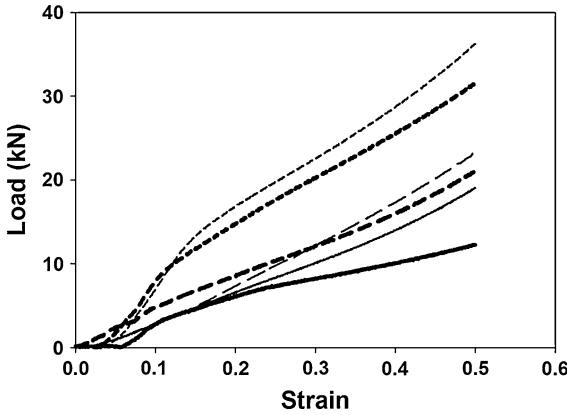

Fig. 7 Rheological properties of the NFC-based aerogels. *Bold lines* represent the aerogels without HAp addition. *Solid line*: AG DO = 0; *long dashed line*: AG DO = 0.1; *short dashed line*: AG DO = 0.2

Conclusions

Nanofibrillated cellulose-based (NFC) aerogels were prepared by vaccum freeze-drying of aqueous suspensions of cellulose nanofibers prepared from high pressure homogenization. As an alternate novel approach to synthesis, the cellulose suspension was successfully modified by TEMPO oxidation after homogenization, and later made bone-biocompatible using hydroxyapatite (HAp) addition to provide aerogels whose chemical and physical properties could be easily tuned by those modifications. The chemical modification of the aerogels caused changes in the morphology, partially due to the nature of the water present in the aerogels as determined by time domain-nuclear magnetic resonance spectroscopy (TD-NMR). NMR studies indicated that carboxylic acid functionalities were able to bind water effectively and thus contribute to a more uniform and larger pores as evidenced from SEM measurements between oxidized and non-oxidized samples. Oxidized aerogels revealed lower densities, whereas the use of HAp increased the density slightly. Morphology of oxidized aerogels presented high pore size homogeneity, which was nearly maintained by the addition of HAp. Both modifications were able to enhance the strength of the aerogels, although oxidation had the most pronounced effect. Mechanically-tuned post-homogenized oxidized NFC-based aerogels are therefore offered as a viable biomaterial platform for further functional applications.

Acknowledgments We would like to gratefully acknowledge the CNPq (Conselho Nacional de Desenvolvimento Científico e Tecnológico) for the generous provision of a research fellowship to TCFS that allowed parts of this work to be realized. The Authors would also like to thank Professor Robert C. Borden from the Department of Civil, Construction and Environmental Engineering for the generous use of the homogenizer.

References

Archer EA, Gong H, Krische MJ (2001) Hydrogen bonding in noncovalent synthesis: selectivity and the directed organization of molecular strands. Tetrahedron 57:1139–1159

Aulin C, Netrval J, Wagberg L, Lindstrom T (2010) Aerogels from nanofibrillated cellulose with tunable oleophobicity. Soft Matter 6(14):3298–3305

Besbes I, Alila S, Boufi S (2011) Nanofibrillated cellulose from TEMPO-oxidized eucalyptus fibres: effect of the carboxyl content. Carbohydr Polym 84(3):975–983

Bragd PL, van Bekkum H, Besemer AC (2004) TEMPO-Mediated oxidation of polysaccharides: survey of methods and applications. Top Catal 27:49–66

Burchell MJ, Creighton JA, Cole MJ, Mann J, Kearsley AT (2001) Capture of particles in hypervelocity impacts in aerogel. Meteorit Planet Sci 36(2):209–221

da Silva Perez D, Montanari S, Vignon MR (2003) TEMPO-Mediated oxidation of cellulose III. Biomacromolecules 4(5):1417–1425

de Nooy AEJ, Besemer AC, van Bekkum H (1995) Highly selective nitroxyl radical-mediated oxidation of primary alcohol groups in water-soluble glucans. Carbohydr Res 269(1):89–98

Dufresne A, Dupeyre D, Vignon MR (2000) Cellulose microfibrils from potato tuber cells: processing and characterization of starch–cellulose microfibril composites. J Appl Polym Sci 76(14):2080–2092

Elder T, Labbé N, Harper D, Rials T (2006) Time domain-nuclear magnetic resonance study of chars from southern hardwoods. Biomass Bioenergy 30(10):855–862

Felby C, Thygesen L, Kristensen J, Jørgensen H, Elder T (2008) Cellulose–water interactions during enzymatic hydrolysis as studied by time domain NMR. Cellulose 15(5):703–710

Gavillon R, Budtova T (2007) Aerocellulose: new highly porous cellulose prepared from cellulose−naoh aqueous solutions. Biomacromolecules 9(1):269–277

Gawryla MD, van den Berg O, Weder C, Schiraldi DA (2009) Clay aerogel/cellulose whisker nanocomposites: a nano-scale wattle and daub. J Mater Chem 19(15):2118–2124

Habibi Y, Chanzy H, Vignon M (2006) TEMPO-mediated surface oxidation of cellulose whiskers. Cellulose 13(6): 679–687

Heath L, Thielemans W (2010) Cellulose nanowhisker aerogels. Green Chem 12(8):1448–1453

Hoepfner S, Ratke L, Milow B (2008) Synthesis and characterisation of nanofibrillar cellulose aerogels. Cellulose 15(1): 121–129

Hong L, Wang YL, Jia SR, Huang Y, Gao C, Wan YZ (2006) Hydroxyapatite/bacterial cellulose composites synthesized via a biomimetic route. Mater Lett 60(13–14):1710–1713

Innerlohinger J, Weber HK, Kraft G (2006) Aerocellulose: aerogels and aerogel-like materials made from cellulose. Macromol Symp 244(1):126–135

Isogai A, Saito T, Fukuzumi H (2011) TEMPO-oxidized cellulose nanofibers. Nanoscale 3(1):71–85

Kwak DH, Hong SJ, Kim DJ, Greil P (2010) The formation of hydroxyapatite on chemically-modified cellulose fibers. J Ceram Process Res 11(2):170–172

Liebner F, Potthast A, Rosenau T, Haimer E, Wendland M (2008) Cellulose aerogels: highly porous, ultra-lightweight materials. Holzforschung 62(2):129–135

Okita Y, Saito T, Isogai A (2010) Entire surface oxidation of various cellulose microfibrils by TEMPO-mediated oxidation. Biomacromolecules 11(6):1696–1700

Paakko M, Vapaavuori J, Silvennoinen R, Kosonen H, Ankerfors M, Lindstrom T, Berglund LA, Ikkala O (2008) Long and entangled native cellulose I nanofibers allow flexible aerogels and hierarchically porous templates for functionalities. Soft Matter 4(12):2492–2499

Park S, Venditti RA, Jameel H, Pawlak JJ (2006) Changes in pore size distribution during the drying of cellulose fibers as measured by differential scanning calorimetry. Carbohydr Polym 66(1):97–103

Saito T, Isogai A (2006) Wet strength improvement of TEMPO-oxidized cellulose sheets prepared with cationic polymers. Ind Eng Chem Res 46(3):773–780

Saito T, Nishiyama Y, Putaux J-L, Vignon M, Isogai A (2006) Homogeneous suspensions of individualized microfibrils from tempo-catalyzed oxidation of native cellulose. Biomacromolecules 7(6):1687–1691

Saito T, Kimura S, Nishiyama Y, Isogai A (2007) Cellulose nanofibers prepared by tempo-mediated oxidation of native cellulose. Biomacromolecules 8(8):2485–2491

Sehaqui H, Allais M, Zhou Q, Berglund LA (2011a) Wood cellulose biocomposites with fibrous structures at micro- and nanoscale. Comp Sci Technol 71(3):382–387

Sehaqui H, Zhou Q, Berglund LA (2011b) Nanostructured biocomposites of high toughness – a wood cellulose nanofiber network in ductile hydroxyethylcellulose matrix. Soft Matter 7(16):7342–7350

Suh DJ, Park T-J (1996) Sol−Gel strategies for pore size control of high-surface-area transition-metal oxide aerogels. Chem Mater 8(2):509–513

Wan YZ, Hong L, Jia SR, Huang Y, Zhu Y, Wang YL, Jiang HJ (2006) Synthesis and characterization of hydroxyapatite-bacterial cellulose nanocomposites. Compos Sci Technol 66(11–12):1825–1832

Wan YZ, Gao C, Luo HL, He F, Liang H, Li XL, Wang YL (2009) Early growth of nano-sized calcium phosphate on phosphorylated bacterial cellulose nanofibers. J Nanosci Nanotechnol 9(11):6494–6500

Zimmermann KA, LeBlanc JM, Sheets KT, Fox RW, Gatenholm P (2011) Biomimetic design of a bacterial cellulose/hydroxyapatite nanocomposite for bone healing applications. Mater Sci Eng C 31(1):43–49